

APPENDIX

Rabaptin5 targets autophagy to damaged endosomes and Salmonella vacuoles via FIP200 and ATG16L1

Valentina Millarte, Simon Schlienger, Simone Kälin, and Martin Spiess*

Table of Contents

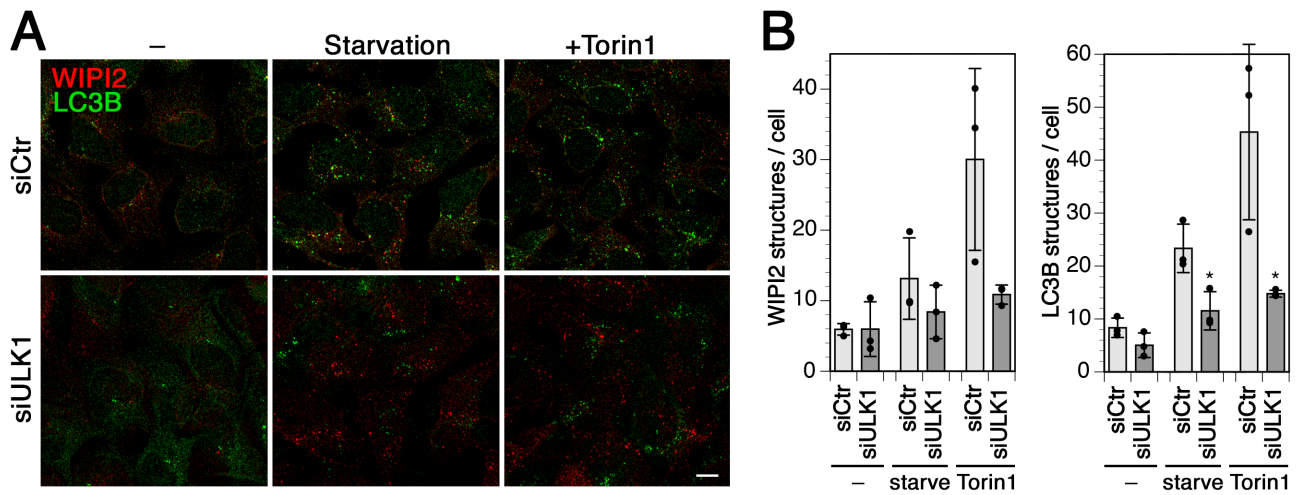
Appendix Table S1.	Rabaptin5 interactors identified by yeast two-hybrid screen.	2
Appendix Figure S1.	ULK1 knockdown inhibits starvation-induced autophagy.	3
Appendix Figure S2.	Silencing of ATG13 or inhibition of ULK1/2 blocks recruitment of ATG16L1 to Rabaptin5-positive endosomes.	4
Appendix Figure S3.	Chloroquine-induced autophagy involves galectin3 and p62 and is independent of BafA1.	5
Appendix Figure S4.	ATG16L1 recruitment to chloroquine-damaged endosomes requires FIP200.	7
Appendix Figure S5.	Deletion of the WD domain in ATG16L1 and the AAA mutation in Rabaptin5 do not abrogate their interaction with FIP200.	8
Appendix Figure S6.	Inactivation of Rabaptin5 does not affect autophagic flux, but chloroquine-induced transferrin receptor degradation.	9

Appendix Table S1. Rabaptin5 interactors identified by yeast two-hybrid screen.

Interaction quality*	Gene name	Protein	Interacting fragment
A	RABEP1	Rabaptin5	579–691
A	RB1CC1	FIP200	281–439
A	VIM	Vimentin	15–144
B	RABGEF1	Rabex5	281–439
B	BARD1	BRCA1-associated ring domain protein 1	47–284
B	GOLGA4	Golgin A4	1116–1281
B	ITSN1	Intersectin 1	554–667
C	SMARCC1	SWI/SNF complex subunit SMARCC1	899–1005

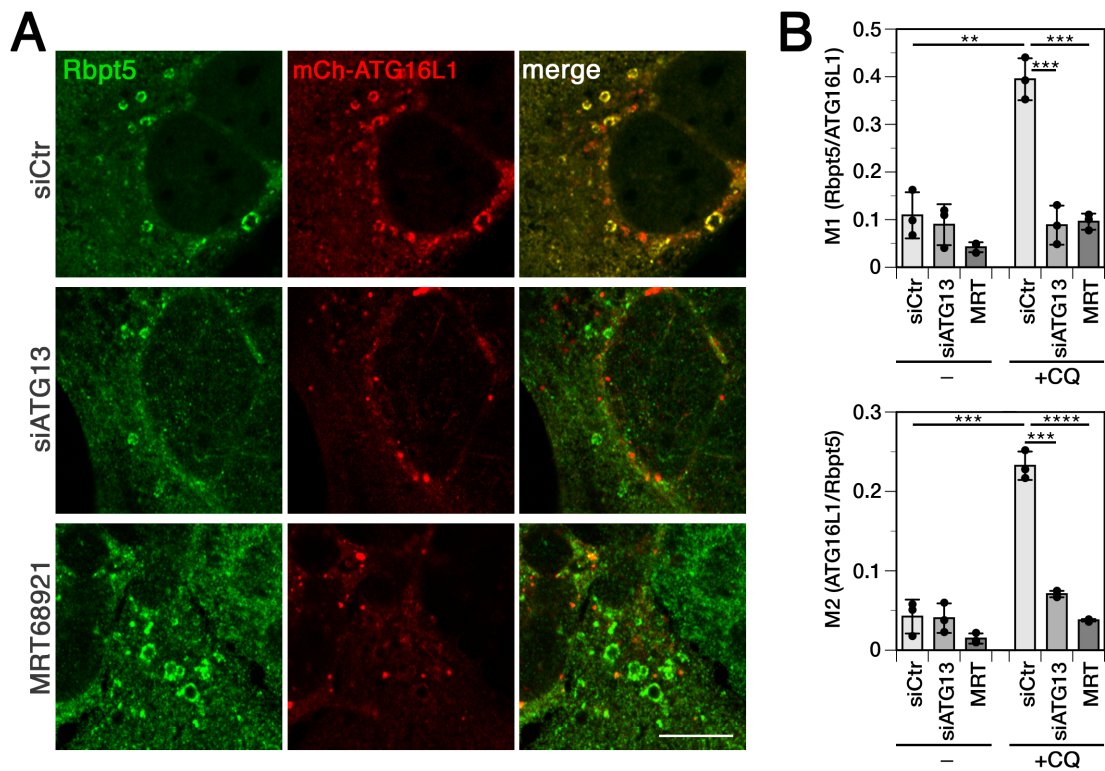
*A–C indicate the confidence level of the interaction from very high to medium.

FIP200, FAK family-interacting protein of 200 kDa; RB1CC1, RB1-inducible coiled-coil protein 1.



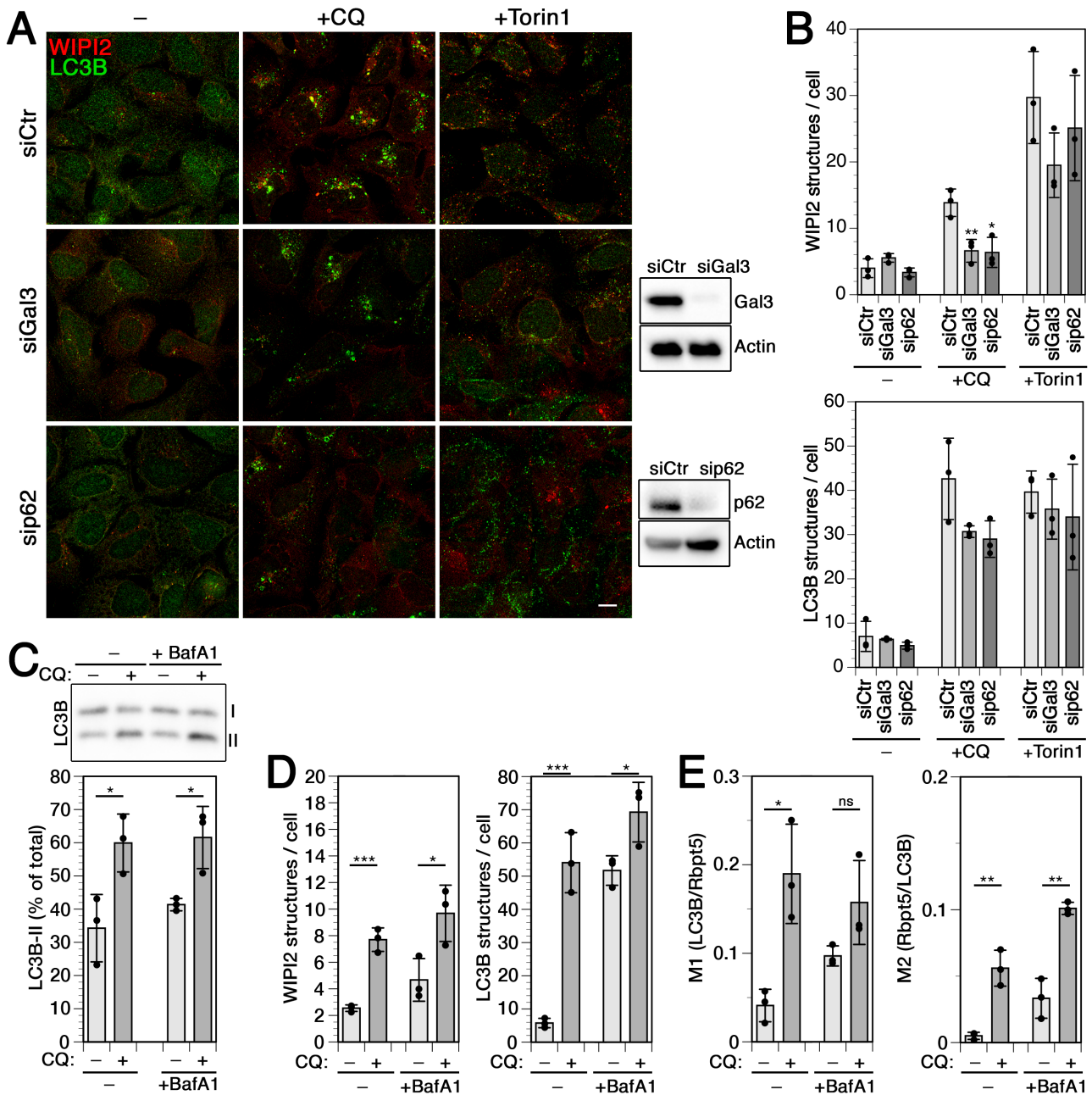
Appendix Figure S1. ULK1 knockdown inhibits starvation-induced autophagy.

- A** HEK293A cells were transfected with nontargeting siRNA (siCtr) or siRNA silencing ULK1 for 72 h as in Fig 4C, and treated without (-) or with 250 nM Torin1 for 150 min, or starved in HBSS medium for 150 min. Cells were fixed and immunostained for endogenous WIPI2 and LC3B. Scale bar, 10 μ m.
- B** WIPI2 or LC3B puncta per cell were quantified for each condition (mean \pm S.D. of three independent experiments; two-tailed Student's t test: * $P < 0.05$).



Appendix Figure S2. Silencing of ATG13 or inhibition of ULK1/2 blocks recruitment of ATG16L1 to Rabaptin5-positive endosomes.

- A** HEK^{+Rbpt5} cells were transfected with nontargeting siRNA (siCtr) or siRNA silencing ATG13 for 72 h and with mCherry-ATG16L1 for 24 h. Cells were treated without (–) or with 60 μ M chloroquine (+CQ) for 30 min, with or without 5 μ M of the ULK1/2 inhibitor MRT68921 (MRT) for 60 min, fixed and stained for Rabaptin5 and mCherry-ATG16L1. Fluorescence micrographs of chloroquine-treated cells are shown. Scale bar, 10 μ m.
- B** Manders' colocalization coefficients were determined for each condition without (–) or with chloroquine (+CQ) or the ULK1/2 inhibitor MRT68921 (MRT), M1 showing the fraction of Rabaptin5-positive structures also positive for mCherry-ATG16L1 and M2 showing the inverse (mean \pm S.D. of three independent experiments; ANOVA: ** P <0.01, *** P <0.001).

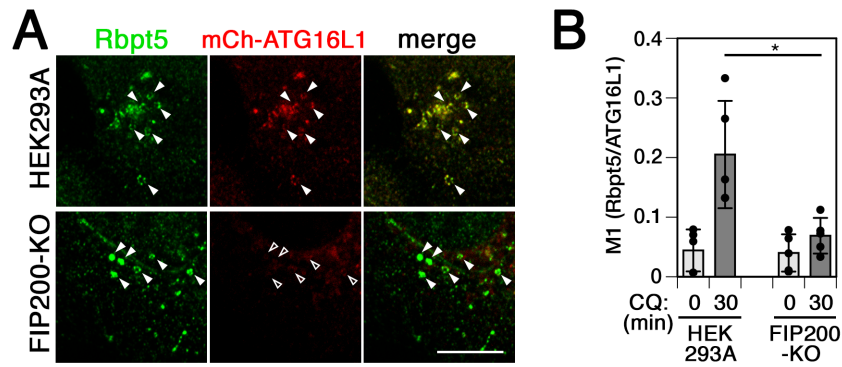


Appendix Figure S3. Chloroquine-induced autophagy involves galectin3 and p62 and is independent of BafA1.

- A** HEK293A cells were transfected with nontargeting siRNA (siCtr) or siRNAs silencing galectin3 (siGal3) or p62 (sip62) for 72 h and treated without (–) or with 60 μ M chloroquine (+CQ) or 250 nM Torin1 for 150 min. Cells were fixed and immunostained for endogenous WIPI2 and LC3B. Scale bar, 10 μ m. Efficiency of galectin3 and p62 knockdown was assayed by immunoblotting.
- B** WIPI2 or LC3B puncta per cell were quantified for each condition (mean \pm S.D. of three independent experiments; two-tailed Student's t test: *P<0.05, **P<0.01).
- C** HEK293A cells were incubated without or with 60 μ M chloroquine and 500 nM BafA1 for 30 min and non-lipidated and lipidated LC3B (I and II, resp.) were assayed by immunoblot analysis. After longer times of incubation with BafA1 and/or chloroquine, lipidation was too strong to differentiate. The fraction of LC3B-II of total LC3B was quantified (mean \pm S.D. of three independent experiments; two-tailed Student's t test: *P<0.05).
- D** HEK293A cells were incubated with or without 60 μ M chloroquine and/or 500 nM BafA1 for 150 min before immunofluorescence localization of WIPI2, LC3B, or Rabaptin5. WIPI2

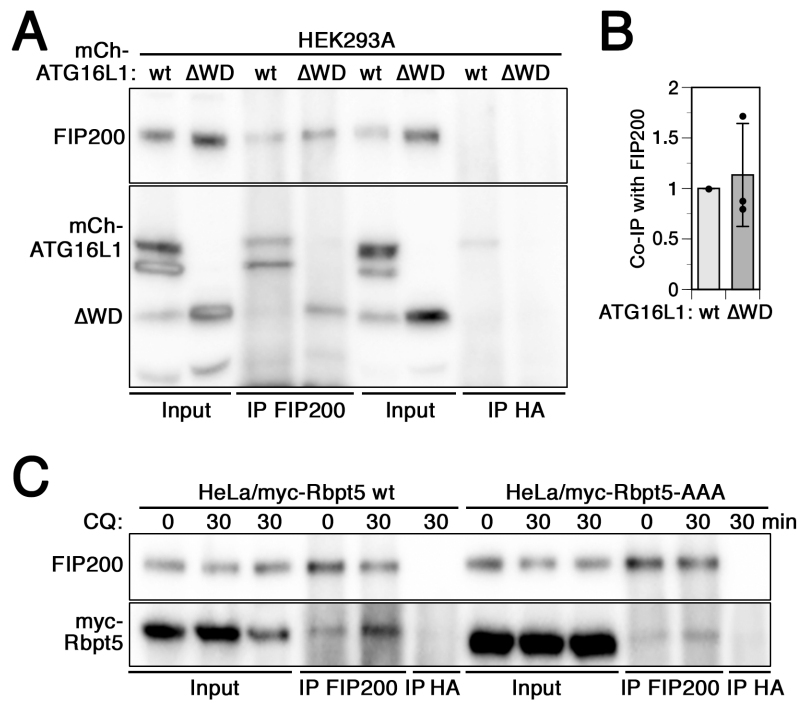
(B) or LC3B puncta per cell (C) were quantified for each condition (mean \pm S.D. of three independent experiments; two-tailed Student's t test: *P<0.05, ***P<0.001).

E Manders' colocalization coefficients were determined, M1 showing the fraction of LC3B-positive structures also positive for Rabaptin5 and M2 showing the inverse. The mean \pm S.D. of three independent experiments is plotted; two-tailed Student's t test: ns not significant, *P<0.05, **P<0.01).



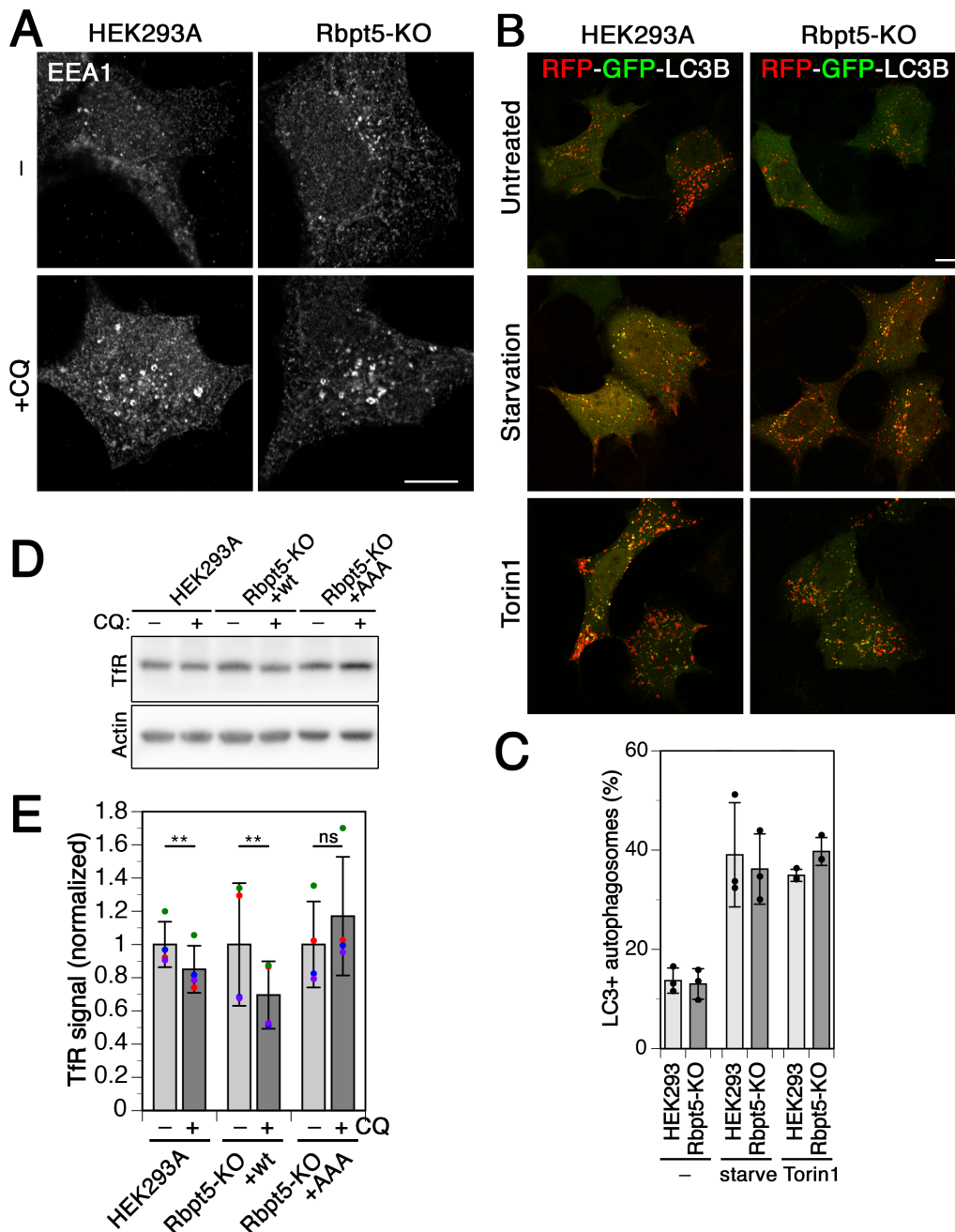
Appendix Figure S4. ATG16L1 recruitment to chloroquine-damaged endosomes requires FIP200.

- A Parental HEK293A and FIP200 knockout cells (FIP200-KO) were transfected with mCherry-ATG16L1 for 24 h and incubated with 60 μ M chloroquine (+CQ) for 30 min and stained for Rabaptin5 and mCherry-ATG16L1. Fluorescence micrographs of chloroquine-treated cells are shown. Scale bar, 10 μ m. Arrowheads point out chloroquine-induced enlarged Rabaptin5-positive early endosomes (empty arrowheads when negative for mCherry-ATG16L1).
- B Manders' colocalization coefficients were determined with and without chloroquine treatment for 30 min. Mean \pm S.D. of five independent experiments; ANOVA: *P<0.05.



Appendix Figure S5. Deletion of the WD domain in ATG16L1 and the AAA mutation in Rabaptin5 do not abrogate their interaction with FIP200.

- A** Lysates of HEK293A cells transiently transfected with full-length mCherry-ATG16L1 (wt) or a mutant lacking the WD domain (Δ WD; residues 1–319 of ATG16L1, precisely deleting only the WD40 repeats residues 320–607) were immunoprecipitated with anti-FIP200 or anti-HA antibodies, and immunoblotted for FIP200 and mCherry-ATG16L1.
- B** Immunoblots as in panel A were quantified (signals normalized to immunoprecipitated FIP200; mean \pm S.D. of three independent experiments each).
- C** HeLa cells transiently transfected with myc-tagged wild-type Rabaptin5 (wt) or triple-alanine mutant (AAA) were incubated for 30 min with or without 60 μ M chloroquine (CQ), lysed, immunoprecipitated with anti-FIP200 (IP FIP200) or anti-HA antibodies (IP HA), and immunoblotted for FIP200 and myc.



Appendix Figure S6. Inactivation of Rabaptin5 does not affect autophagic flux, but chloroquine-induced transferrin receptor degradation.

- A** HEK293A and Rabaptin5-KO cells were treated without and with 60 μ M chloroquine for 30 min and immunostained for EEA1-positive early endosomes. Endosome swelling is independent of Rabaptin5. Scale bar, 10 μ m.
- B** HEK293A cells and Rabaptin5-KO cells were transduced to express tandem fluorescent RFP-GFP-LC3, starved in HBSS medium or treated with 250 nM Torin1 for 150 min, fixed and subjected to fluorescence microscopy. Scale bar, 10 μ m.
- C** The number of autophagosomes (GFP+/RFP+) and autolysosomes (GFP-/RFP+) were counted and autophagosomes plotted as a percentage of the total (mean \pm S.D. of three independent experiments quantifying at least 16 cells per condition).
- D** The indicated cell lines were incubated with or without 60 μ M chloroquine (CQ) overnight before immunoblot analysis for (TfR) and actin.

E The transferrin receptor signal of immunoblots as in panel D was quantified and normalized to actin. The mean \pm S.D. of four independent experiments (indicated by colors) is shown; two-tailed, paired Student's t test: ns not significant, **P<0.01).